One-Parameter Superscaling at the Metal-Insulator Transition in Three Dimensions

Imre Varga,[1,2] Etienne Hofstetter,[3] and János Pipek[1]
[1]*Elméleti Fizika Tanszék, Budapesti Műszaki Egyetem, H-1521 Budapest, Hungary*
[2]*Fachbereich Physik, Philipps-Universität Marburg, Renthof 6, D-35032 Marburg an der Lahn, Germany*
[3]*Blackett Laboratory, Imperial College, London SW7 2BZ, United Kingdom*
(Received 17 October 1997; revised manuscript received 8 December 1998)

Based on the spectral statistics obtained in numerical simulations on three-dimensional disordered systems within the tight-binding approximation, a new superuniversal scaling relation is presented that allows us to collapse data for the orthogonal, unitary, and symplectic symmetries ($\beta = 1, 2, 4$) onto a single scaling curve. This relation provides strong evidence for one-parameter scaling existing in these systems which exhibit a second order phase transition. As a result a possible one-parameter family of spacing distribution functions, $P_g(s)$, is given for each symmetry class β, where g is the dimensionless conductance. [S0031-9007(99)09296-0]

PACS numbers: 71.30.+h, 05.60.Gg, 72.15.Rn

The study of critical phenomena is an important subject because of the rich variety of systems exhibiting a second order phase transition [1]. By a second order transition we mean a continuous transition between two regimes with the correlation length diverging at the transition point. The description of such a phenomenon leads to the introduction of very important concepts such as scaling, renormalization group, and universality classes. These reflect the fact that the phase transition does not depend on the details of the system but only on some general symmetries as well as on the dimension of the system. A direct consequence is that different systems with different Hamiltonians may share the same critical exponents, describing the singularity of the phase transition, if the symmetry underlying these systems is the same and therefore will belong to the same universality class. Other features, on the other hand, may be in common for different universality classes leaving the possibility to derive simple relations between these classes. Such a feature is scaling which is exploited in order to find the position of the critical point and the value of the critical exponent. Even though scaling may be commonplace, the scaling function may be different for the different universality classes.

In this Letter we present a single one-parameter scaling relation which is common to several different universality classes. This relation involves the spectral statistics of a three-dimensional (3D) disordered system with additional degrees of freedom, e.g., strong magnetic field and spin-orbit scattering. The choice of this system comes from the realization that it exhibits a metal-insulator transition (MIT) as a function of the disorder in the thermodynamic limit [2]. It is generally assumed that the critical behavior at the MIT can be classified in terms of three different universality classes according to the symmetry of the system: orthogonal [with time reversal symmetry, O(N)], unitary [without time reversal symmetry, e.g., with a magnetic field, U(N)] and, symplectic [with spin-orbit coupling, Sp(N)]. One then expects different critical exponents related to the MIT for the three different universality classes.

Surprisingly, in spite of the apparent change of universality class, the same value of the critical exponent has been found, numerically, both in the presence and absence of a magnetic field [3,4], as well as spin-orbit coupling [5,6]. Moreover, Ohtsuki *et al.* recently showed [7] that the anomalous diffusion exponent and also the fractal dimension $D(2)$ seem to coincide at the MIT for O(N), U(N), or Sp(N), in agreement with these results. It was recently proposed [6,8] that a natural way to understand these coincidences would be to invoke the spontaneous breaking of the symmetry right at the MIT. However, in a recent paper [9], numerical evidence has been presented suggesting a small difference between the scaling properties of orthogonal and unitary systems.

The problem is therefore far from being solved and we wish to present new evidence concerning how the different universality classes are linked together. This indication gives a nontrivial hint about the way in which the symmetry parameter enters into the scaling function valid for each individual universality class. We also present a possible one-parameter family of spacing distribution functions, $P(s)$, for each universality class.

A convenient way to study the MIT is to resort to random matrix theory (RMT) and energy level statistics (ELS) [10–12]. In RMT the statistics of the energy spectrum are generally described by three different ensembles, Gaussian orthogonal (GOE), unitary (GUE), and symplectic (GSE) depending upon the symmetries mentioned above. Recently it has been shown [5,6,8,10,13,14] that in addition to the two expected statistics, namely, either GOE, GUE, or GSE for the metallic regime and the Poisson ensemble (PE) for the insulating regime, there is a third statistics, called the critical ensemble, which occurs only exactly *at* the critical point.

In order to investigate the MIT we consider the following tight-binding Hamiltonian [2]

$$H = \sum_n \epsilon_n |n\rangle\langle n| + \sum_{n,m} V_{n,m} |n\rangle\langle m| \tag{1}$$

with

$$V_{n,m} = \begin{cases} V, & \text{orthogonal,} \\ V \exp(i\theta_{n,m}), & \text{unitary,} \\ V \exp(i\boldsymbol{\theta}_{n,m}), & \text{symplectic,} \end{cases} \tag{2}$$

where the sites n are distributed regularly in 3D space, e.g., on a simple cubic lattice. Only nearest neighbor interactions are considered. The phase $\theta_{n,m}$ is a scalar related to the magnetic field [8] and $\boldsymbol{\theta}_{n,m}$ is a 2×2 matrix [6]. The site energy ϵ_n is described by a stochastic variable. In the present investigation we use a box distribution with variance $W^2/12$. The parameter W describes the disorder strength and is the critical parameter.

Based on the above Hamiltonian, the MIT is studied by the ELS method, i.e., via the fluctuations of the energy spectrum [6,10]. Starting from Eq. (1) the energy spectrum was computed by means of the Lanczos algorithm for systems of size $L \times L \times L$ with $L = 13$, 15, 17, 19, and 21 and W ranging from 3 to 100 averaging over different realizations of the disorder. After unfolding the spectra obtained, the fluctuations can be appropriately described by means of the spacing distribution $P(s)$ [11]. This distribution measures the level repulsion and is normalized as is its first moment: $\mu_1 = \langle s \rangle = 1$.

In order to characterize the shape of $P(s)$, we first calculate shape descriptive parameters which continuously change as we vary external parameters, e.g., the system size L or disorder W:

$$q = \mu_2^{-1} \quad \text{and} \quad S_{\text{str}} = \mu_S + \ln\mu_2 , \tag{3}$$

where $\mu_2 = \langle s^2 \rangle$ is the second moment of $P(s)$, while $\mu_S = -\langle s \ln s \rangle$. These quantities were first introduced to describe the spatial-localization properties of general lattice distributions [15] and then used for the shape analysis of $P(s)$ around the MIT [16]. It is interesting to note that in contrast to previous methods which used only part of the information contained in $P(s)$ [10,13] we consider here the entire distribution obtained numerically. Parameter q is a well-known quantity in probability theory that describes the peakedness of a distribution function. For example, for $P(s) = \delta(s - 1)$ we have $q = 1$. The parameter S_{str} is called the structural entropy for reasons described elsewhere [15]. These parameters describe not only the bulk features of $P(s)$, but also they are sensitive to the numerical upper cutoff of the support of $P(s)$.

In order to describe and compare the different universality classes within the same method we perform a linear rescaling as

$$-\ln(q) \to \frac{-\ln(q) + \ln(q_W)}{-\ln(q_P) + \ln(q_W)} = \tilde{Q} , \tag{4a}$$

$$S_{\text{str}} \to \frac{S_{\text{str}} - S_W}{S_P - S_W} = \tilde{S} , \tag{4b}$$

where index P refers to the PE and W to the Wigner surmise representing the GOE, GUE, or GSE, respectively. Their values are listed in Table I. The choice of such a rescaling defined in Eqs. (4a) and (4b) maps the variables $\tilde{S}$ and $\tilde{Q}$ onto the $[0, 1]$ interval, with $\tilde{S} = Q = 0(1)$ belonging to the RMT (PE) limit. Furthermore, in Eq. (4a) it is more natural to use $-\ln(q)$ instead of q since, similarly to S_{str}, it is connected to differences of Rényi entropies [17]. As an illustration of the behavior of these parameters, in Fig. 1 we report the results for $\tilde{Q}(L, W)$ and $\tilde{S}(L, W)$ for the case of spin-orbit coupling ($\beta = 4$). We can see that the data depend on the size of the system except at the critical point W_c where $P(s)$ is scale invariant. This is due to the fact that the MIT is a second order transition and that finite-size scaling laws apply close to the transition [18]. These properties were already used with success to describe the MIT [10,13,19]. In particular, it was shown that such quantities have a finite-size scaling behavior and can be written as

$$q(L, W) = f(L/\xi_\infty); \qquad S_{\text{str}}(L, W) = h(L/\xi_\infty) \tag{5}$$

with correlation length $\xi_\infty(W) \sim |W - W_c|^{-\nu}$, and the critical exponent ν. The functions $f(x)$ and $h(x)$ are universal in the sense that they do not depend on the details of the systems—just on the general symmetries—and therefore they directly reflect the universality class of the system.

From Eq. (5) we can see that, because of the scaling behavior of $q(L, W)$ and $S_{\text{str}}(L, W)$, if we plot S_{str} as a function of q we can see the similarities and also the differences between the universality classes. The same is true for the rescaled parameters $\tilde{Q}$ and $\tilde{S}$.

Indeed, Fig. 2 shows clear differences between the orthogonal, unitary, and symplectic cases, although all the data fall onto special curves irrespective of W and L for each case. This figure allows us to determine the scaling relations for $\beta = 1$, 2, and 4 without having to derive $f(L/\xi_\infty)$, $h(L/\xi_\infty)$, and $\xi_\infty(W)$ which are not easy to obtain numerically due to their singularities at the critical point. Using now the rescaling defined above in Eqs. (4a) and (4b), we plot $\tilde{S}(L, W)$ as a function of $\tilde{Q}(L, W)$. The results are shown in Fig. 3. We see that all the data scale nicely onto the *same* curve indicating the presence of a one-parameter superscaling function. The position of the MIT moves along the *same* curve, for $\beta = 1, 2$, and 4, as a function of the critical disorder W_c which can be changed by the magnetic field and spin-orbit scattering

TABLE I. Shape descriptive parameters for the case of different $P(s)$ functions.

	Poisson	GOE	GUE	GSE	$\delta(s - 1)$
β	0	1	2	4	∞
q	0.5295	0.7854	0.8488	0.9054	1.0
$-\ln(q)$	0.6358	0.2416	0.1639	0.0994	0.0
S_{str}	0.2367	0.1025	0.0733	0.0464	0.0

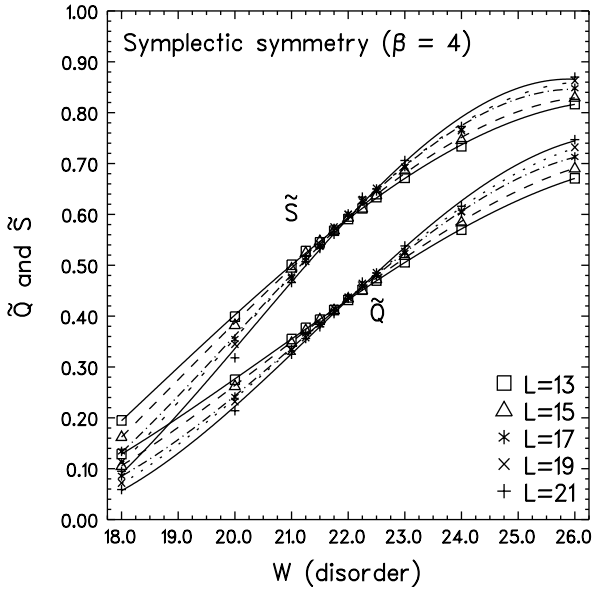

FIG. 1. $\tilde{Q}(L,W)$ and $\tilde{S}(L,W)$ for the case of symplectic symmetry. Continuous curves are polynomial fits.

rate as well as the type of potential scattering. This new superscaling relation is very interesting and of importance in shedding new light on the MIT in 3D systems. New results [21] indicate that the data for $\beta = 2$ in 2D scale onto a different curve (see Fig. 3). This point is important because it implies that superscaling is not a mere consequence of the universality of level repulsion but something more subtle.

Next we will show that the observed relation $\tilde{S}(\tilde{Q})$ presented in Fig. 3 can be understood with the introduction of the dimensionless conductance as a scaling variable. We have found that the constant shifts in (4) for both terms $-\ln(q) + \ln(q_W)$ and $S_{\rm str} - S_W$ correspond to a convolution of different distributions [22]:

$$\mathcal{P}_{g,\beta}(e^x) = \int_{-\infty}^{\infty} \mathcal{Q}_{g,\beta}(e^{x-y})\,\mathcal{W}_\beta(e^y)\,dy \qquad (6)$$

with $e^x \equiv s$. In this case [22] $-\ln(q_{\mathcal{P}}) = -\ln(q_{\mathcal{Q}}) - \ln(q_{\mathcal{W}})$ and also $S^{\mathcal{P}}_{\rm str} = S^{\mathcal{Q}}_{\rm str} + S^{\mathcal{W}}_{\rm str}$.

In Eq. (6), $\mathcal{P}_{g,\beta}(s)$ is the numerically obtained spacing distribution for different symmetry classes parametrized by the dimensionless conductance g, which ranges from zero to infinity as L and W change as well, and $\mathcal{W}_\beta(t)$ is the RMT limit for $g \to \infty$ represented by, e.g., the Wigner surmise. This rescaling provides us with a method to study what is *beyond* the universal level repulsion present in finite systems in the full range of disorder. The parameters $-\ln(q)$ and $S_{\rm str}$ of $\mathcal{P}_{g,\beta}(s)$ give different curves (see Fig. 2), while after rescaling $\tilde{Q}$ and $\tilde{S}$ give the *same* curve (see Fig. 3). This is what is meant by the *superscaling* relation as can be seen in Fig. 3. Scaling in this context refers to the appearance of g. We will show that the parameters $\tilde{Q}$ and $\tilde{S}$ of the function $\mathcal{Q}_{g,\beta}(s)$ appearing in Eq. (6) can account for the major part of the numerically observed relation.

In what follows we give an approximate formula for $\mathcal{P}_{g,\beta}(s)$ based on analytical calculations and a phenomenological assumption. First, we point out that Eq. (6) can

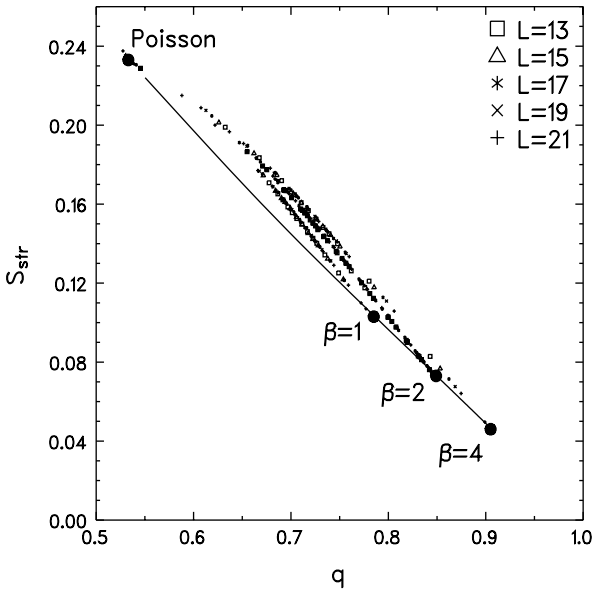

FIG. 2. $S_{\rm str}$ as a function of q for all the symmetry classes. (All data are presented in the full range of disorder.) The solid curve is obtained from a simple interpolating $P(s)$ due to Izrailev [20]. The RMT and Poisson distributions appear as solid circles using the values of Table I.

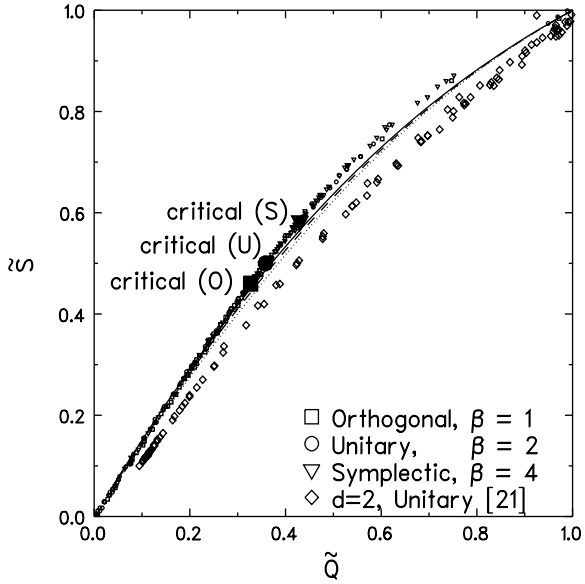

FIG. 3. $\tilde{S}(L,W)$ as a function of $\tilde{Q}(L,W)$ for all the symmetry classes. The solid symbols represent the positions of the critical points. The continuous (solid, dashed, and dotted lines) curves are our analytical estimates (see text for details). For comparison, the results obtained for the network model [21] of the quantum Hall effect ($d = 2$, $\beta = 2$) are also presented.

be solved exactly for the extreme cases of a perfect metal ($g \to \infty$) and perfect insulator ($g \to 0$). In the former case the left hand side should equal the Wigner surmise and it is easy to show that such a convolution will hold if the $\mathcal{Q}_{g,\beta}(s)$ function as $g \to \infty$ approaches a Dirac-delta function, $\delta(s-1)$. As for the perfect insulator we have to find $\mathcal{Q}_{0,\beta}$ so that the left hand side in each case equals $P(s) = \exp(-s)$. The solution for these problems, introducing the notation $R(s) \equiv \mathcal{Q}_{0,\beta}(s)$, is [22]

$$R(y) = a \begin{cases} e^{-y^2} & \beta = 1, \\ \mathrm{erfc}(y) & \beta = 2, \\ (2y^2+1)\,\mathrm{erfc}(y) - \frac{2y}{\sqrt{\pi}} e^{-y^2}, & \beta = 4, \end{cases} \tag{7}$$

where $y = bs$, $a = 2/\pi$, $\pi/4$, and $9\pi/64$, and $b = 1/\sqrt{\pi}$, $\sqrt{\pi}/4$, and $3\sqrt{\pi}/16$ for $\beta = 1$, 2, and 4, respectively.

These solutions are spacing distributions themselves since their zeroth and first moments are normalized to unity. The interpolating formula is introduced based on the most simple assumption

$$\mathcal{Q}_g(s) = a_g s^g R(b_g s). \tag{8}$$

Parameters a_g and b_g are determined from the normalization conditions $\langle 1 \rangle = \langle s \rangle = 1$ for each β. These interpolating distributions behave in the limit $g = 0$ and $g \to \infty$ appropriately as defined above. The continuous curves in Fig. 3 show that the rescaled Rényi entropies of $\mathcal{Q}_g(s)$ [Eq. (8)] indeed reproduce the results of the numerical experiments. Solid, dashed, and dotted lines stand for $\beta = 1$, 2, and 4, respectively. However, we see that the analytical curves do *not* fall onto the same curve. This discrepancy may be due to the simplicity of the approximation in (8) and also because of the presence of a maximal spacing, i.e., a cutoff in both the numerical histogram and consequently in the analytical curves. The analytical curves without the upper cutoff (not presented here) fall on top of each other within the linewidth precision.

Finally, Fig. 3 allows us to give an estimate of the critical conductance g^*. The best fits to the numerical histograms give $g^* = 1.58$, 1.46, and 1.34 for $\beta = 1$, 2, and 4, respectively.

In conclusion, we have presented evidence for a new superscaling relation characterizing the MIT in 3D disordered systems with different additional degrees of freedom, i.e., in different universality classes. Such a relation gives a hint for the derivation of the symmetry dependence of the scaling function. We have also given an approximate analytical formulation of the spacing distribution where the symmetry parameter β and the scaling variable g enter in a very clear way. The estimates of the critical conductance on the other hand show differences for the position of the MIT. This result is complementary to the fact that the critical exponent ν obtained numerically in the three cases is the same [3–6].

We have to note that in some recent experiments providing the same value of the critical exponent [23,24], as well as the absence of the influence of the magnetic field [24] and the spin-orbit coupling [23] at the MIT, show the possibility that the superscaling relation presented in this Letter could be verified experimentally.

The method presented in this Letter can be useful in the analysis of other phase transitions as well.

We thank M. Blencowe for reading the manuscript. Financial support from Országos Tudományos Kutatási Alap (OTKA), Grants No. T029813, No. T024136, and No. F024135 are gratefully acknowledged.

[1] J. J. Binney *et al.*, *The Theory of Critical Phenomena* (Oxford University Press, New York, 1992).
[2] B. Kramer and A. MacKinnon, Rep. Prog. Phys. **56**, 1469 (1993), and references therein.
[3] T. Ohtsuki *et al.*, J. Phys. Soc. Jpn. **62**, 224 (1993).
[4] M. Henneke *et al.*, Europhys. Lett. **27**, 389 (1994).
[5] T. Kawarabayashi *et al.*, Phys. Rev. Lett. **77**, 3593 (1996).
[6] E. Hofstetter, Phys. Rev. B **57**, 12 763 (1998).
[7] T. Ohtsuki and T. Kawarabayashi, J. Phys. Soc. Jpn. **66**, 314 (1997).
[8] E. Hofstetter, Phys. Rev. B **54**, 4552 (1996); E. Hofstetter and M. Schreiber, Phys. Rev. Lett. **73**, 3137 (1994).
[9] K. Slevin and T. Ohtsuki, Phys. Rev. Lett. **78**, 4083 (1997).
[10] B. I. Shklovskii *et al.*, Phys. Rev. B **47**, 11 487 (1993).
[11] Th. Guhr *et al.*, Phys. Rep. **299**, 189 (1998).
[12] B. L. Alt'shuler and B. I. Shklovskii, Sov. Phys. JETP **64**, 127 (1986).
[13] E. Hofstetter and M. Schreiber, Phys. Rev. B **48**, 16 979 (1993).
[14] M. Batsch *et al.*, Phys. Rev. Lett. **77**, 1552 (1996); I. Zharekeshev and B. Kramer, Phys. Rev. Lett. **79**, 717 (1997).
[15] J. Pipek and I. Varga, Phys. Rev. A **46**, 3148 (1992).
[16] I. Varga, *et al.*, Phys. Rev. B **52**, 7783 (1995).
[17] J. Pipek and I. Varga, Int. J. Quantum Chem. **64**, 85 (1997).
[18] M. E. Fisher and M. N. Barber, Phys. Rev. Lett. **28**, 1516 (1972).
[19] E. Hofstetter and M. Schreiber, Phys. Rev. B **49**, 14 726 (1994).
[20] F. Izrailev, J. Phys. A **22**, 865 (1989).
[21] M. Metzler and I. Varga, J. Phys. Soc. Jpn. **67**, 1856 (1998).
[22] J. Pipek and I. Varga (to be published).
[23] H. Stupp *et al.*, Phys. Rev. Lett. **71**, 2634 (1993).
[24] M. Hornung *et al.*, Europhys. Lett. **28**, 43 (1994).